CHAPTER 4

Image-Guided Procedures: Tools, Techniques, and Clinical Applications

Cristian A. Linte[1], John T. Moore[2], Elvis C.S. Chen[2], Terry M. Peters[2]
[1]Biomedical Engineering and Center for Imaging Science, Rochester Institute of Technology, Rochester, NY, USA; [2]Imaging Research Laboratories, Robarts Research Institute, Western University, London, ON, Canada

4.1 BACKGROUND AND INTRODUCTION

Most surgical procedures and therapeutic interventions traditionally were only possible by gaining direct access to the internal anatomy using direct visual inspection to deliver therapy and treat the condition. Using this approach, several medical imaging modalities have been used to diagnose the condition, plan the procedure, and monitor the patient during the surgery, but the tissue manipulation and delivery of therapy has been performed under invasive incisions to give direct visualization of the surgical site and ample access inside the body. Over the past two decades, significant efforts have been dedicated to minimizing the invasiveness associated with surgical interventions, which has been made possible by advancements in medical imaging, surgical navigation, visualization, and display technologies.

Modern image-guided interventions (IGI) or image-guided surgical techniques have now been in use for approximately 30 years, beginning with stereotactic brain surgery and are slowly becoming used in orthopedic, spinal, cardiac, and abdominal areas. As highlighted by Galloway and Peters [1], an image-guided procedure comprises five distinct steps, namely, the acquisition of preoperative data, generally in the form of tomographic images; the localization and tracking of the position of the surgical tool or therapeutic device; registration of a localized volume with the preoperative data; intuitively displaying the position of the tool with respect to medically important structures visible in the preoperative data; and taking into account the differences between the preoperative data and the patient during surgery. The successful implementation of an image-guided surgical platform must integrate these steps within a single platform. In many cases,

Bioengineering for Surgery
ISBN 978-0-08-100123-3
http://dx.doi.org/10.1016/B978-0-08-100123-3.00004-X

preoperative images are complemented with intraoperative imaging, whose broad definition also includes the acquisition of electrophysiological data in addition to traditional "imaging" modalities.

Computers have become an integral part of medicine, enabling the acquisition, processing, analysis, and visualization of medical images and their integration into diagnosis and therapy planning [2], surgical training [3–6], pre- and intraoperative data visualization [7–9], and intraoperative navigation [10–13]. These technologies have allowed clinicians not only to perform procedures that were rarely successful decades ago, but also to embrace the use of less invasive techniques to reduce procedure morbidity and patient trauma.

In addition to providing diagnosis, medical imaging also has enabled several minimally invasive procedures; however, the success of the procedure depends upon the clinician's ability to mentally recreate the view of the surgical scene based on the intraoperative images. These images provide only a limited field of view of the internal anatomy, and also are of lower quality and with reduced field of view compared with the preoperative images used for diagnosis. Moreover, depending on the imaging modality used, the surgical instruments used during therapy may not easily be depicted in the intraoperative images, raising the need for additional information.

To provide accurate guidance of the surgical tool to the target while avoiding critical anatomical structures, several data types acquired from different sources at different stages of the procedure need to be integrated within a common image guidance workflow. High-quality preoperative images and anatomical models can be used to provide the "big picture" of the internal anatomy that help the surgeon navigate from the point of access to the target to be treated, to serve as a road map. The used surgical tools typically are instrumented with tracking (i.e., localization) sensors that encode the tool position and orientation. If the patient anatomy is registered to the preoperative images/models (typically achieved via the tracking system), the virtual representation of the surgical instruments can be visualized in the same coordinate system as the road map, in a similar fashion to using a global positioning navigation system to obtain positioning information along a route. To compensate for the limited intraoperative faithfulness provided by the "slightly outdated" preoperative data, intraoperatively acquired images also are integrated into the image guidance environment. This provides accurate and precise target identification and on-target instrument positioning based on real-time information. After fusion of the pre- and intraoperative images and instrument tracking information, the physician performs the tool-to-target navigation using

the preoperative images/models augmented with the virtual tool representations. This is followed by the on-target instrument positioning under real-time image guidance complemented by real-time instrument tracking.

The multimodality guidance and navigation information can be displayed to the surgeon via traditional two-dimensional (2D) display screens available in the interventional suites in the form of an augmented reality display. This is either directly overlaid onto the patient's skin (i.e., optical-based augmented reality) or by augmenting a video display of the patient (i.e., video-based augmented reality) via tracked head-mounted (stereoscopic) displays, or recently developed and commercially available three-dimensional (3D) displays [14].

4.2 COMMON COMPONENTS OF IMAGE GUIDANCE PLATFORMS

4.2.1 Medical Imaging Modalities

Medical images are typically acquired for diagnostic purposes and often their value is minimal during the treatment of the condition should a surgical intervention be required. However, when using minimally invasive approaches to therapy, ample direct vision is not an option and images acquired during the diagnostic stage become a critical component to guide the procedure. The role of high-quality tomographic scans such as computed tomography (CT) or magnetic resonance imaging (MRI) is two-fold: to assist in the planning of the procedure and to provide the larger anatomical context during the procedure.

4.2.1.1 Computed Tomography

CT generates 3D representations of the internal anatomy based on the density of the tissues encountered by the X-rays [15]. Latest generation CT scanners can acquire high-resolution 3D volumetric images of the abdomen and thoracic cavity in several seconds, and also allow for "cine" imaging and dynamic visualization of the beating heart. However, given the rather similar density, most soft tissues cannot easily be differentiated and so radiopaque contrast agents are typically used to enhance these structures.

4.2.1.2 Magnetic Resonance Imaging

MRI provides maps of the anatomy by imaging the response of protons present in different types of tissues to magnetic excitations of variable duration across different spatial directions [16]. As such, MRI acquisition is

not restricted to the axial direction. Furthermore, given that the water molecules in different tissues are exposed to a slightly different magnetic environment, the MRI soft-tissue imaging capabilities are superior to those of traditional CT without the use of contrast enhancement. Given their high resolution, soft-tissue imaging capabilities and large field of view, these tomographic image datasets are preprocessed to extract the patient-specific anatomy in the region of interest (i.e., the surgical target to be treated), to determine the optimal path to reach that target, and to provide the "bigger picture" of the anatomy to interpret the intraoperative images.

Despite their benefits, most CT and MRI datasets are preoperative or diagnostic in nature, given that their acquisition has been several days before the intervention. This limits their direct intraoperative use because of the inherent anatomical and physiological difference between the pre- and intraoperative conditions (e.g., organ shift because of slightly different patient position). To accurately depict the intraoperative anatomy, real-time imaging is crucial and complements the already available preoperatively depicted anatomy. Modalities such as X-ray and ultrasound (US) imaging have long been used as simple, inexpensive, and feasible approaches to "see" internal anatomy, and currently both these modalities are used to monitor and visualize therapy delivery during procedures.

4.2.1.3 X-Ray Imaging

X-ray fluoroscopy has been used in percutaneous catheter-navigation procedures for almost two decades because of its ability to depict surgical instruments such as guidewires, catheters, and other implantable devices such as stents and valves, but it has inherent limitations associated with soft tissue visualization.

An extension of traditional X-ray fluoroscopy are the recently developed cone-beam CT systems [17–19], which enable real-time imaging and 3D reconstruction of anatomical structures intraoperatively, therefore reducing the reliance on preoperative CT scans and providing superior visualization to traditional X-ray fluoroscopy.

4.2.1.4 Ultrasound

US makes images of the anatomy by mapping the amplitude and arrival time of the reflected sound waves to image intensity and axial distance, respectively. Although used mainly for diagnostic purposes, US has been adopted more recently for intraoperative monitoring and guidance, because of its noninvasive, versatile, portable, low-cost, and real-time capabilities.

US images can be acquired from the body surface, for example, by using transthoracic probes for cardiac imaging, or from closer to the organ of interest by using transesophageal or intracardiac probes, or from laparoscopic, transperineal, or intravascular probes, thereby minimizing attenuation while maintaining resolution during real-time imaging. US imaging has evolved from simple 2D images to 3D and four-dimensional (3D + time) acquisitions, providing live "cine" imaging capabilities of moving structures, such as valve leaflets. In addition, by determining the position and orientation of the US probe using tracking technologies (described in the next section), the emerging images can be displayed alongside preoperative imaging data together with virtual representations of the surgical tools. This adds context to the otherwise "context-less" 2D or 3D US images and facilitates tool-to-target navigation and on-target positioning.

4.2.1.5 Nuclear Imaging

A somewhat different class of medical images is represented by nuclear imaging modalities, such as positron emission tomography and single photon emission CT. Both of these modalities are typically used to image metabolic processes in regions of interest, and for more intuitive interpretation they are typically registered (or intrinsically coregistered by means of dual imaging systems such as positron emission tomography-CT or positron emission tomography-MRI) to morphological images such as CT and MRI. Although still in their infancy, recent studies have reported efforts to integrate nuclear imaging with intraoperative laparoscopic technology, enabling functional and metabolic assessment in near real-time during therapy delivery.

4.2.2 Image Manipulation: Segmentation, Registration, Fusion

Often it is possible to provide clinicians with additional or enhanced image information not inherently present intraoperatively. Modalities such as CT and MRI are not typically available in the operating room, but are often the optimal source for clearly identifying target tissues. In such situations, the best approach is to register the preoperative image data with the intraoperative modalities, as for example during prostate biopsies [20].

In other cases, performance of surgical tasks can be made more intuitive with the fusion of intraoperative modalities such as endoscopy and US. Although each modality is present intraoperatively, the process of placing

them in a common reference frame can add a substantial cognitive load on the clinician. By registering US devices with video cameras, either by using the tracking technologies described later in "Surgical Tracking" or by using video image-based tracking of the US transducer, it is possible to fuse these modalities into a common coordinate frame (see Chapter 3).

Surface segmentation also can play a valuable role in IGI as a means of highlighting anatomical landmarks for surgical targets, or simply providing convenient reference points for interpreting image data. Because parallel computing is becoming ever more robust, near real-time segmentation of intraoperative image data has become increasingly feasible.

4.2.3 Surgical Localization and Tracking

Because the surgical scene is not directly visible during most minimally invasive interventions, the position and orientation of the surgical instrument with respect to the target and surrounding anatomy must be precisely known at all times during the procedure. To address this requirement, spatial localizers have become an integral part of image-guided navigation platforms, enabling the tracking of all interventional tools within the same coordinate system attached to the patient.

Optical and magnetic (also referred to as "electromagnetic") tracking are the localization technologies most commonly used in IGI. Although optical tracking systems are known for their superior accuracy when compared with most magnetic localizers, they do require an unobstructed line of sight between the transmitting device and the optical sensors mounted on the tracked instrument, therefore preventing their use as tracking tools inside the body. Optical tracking systems are typically used for procedures in which the tracked rigid instruments extend outside the body, with the exception of endoscopic procedures, in which the endoscopic video used for visualization provides vision-based tracking.

Magnetic tracking systems (MTS), on the other hand, do not suffer from the line-of-sight limitation and provide a versatile solution when tracking flexible instruments inserted inside the body, such as catheters, endoscopes, and/or laparoscopes, or US imaging probes. However, because these systems rely on magnetic fields to encode the position and orientation of the tracked instrument, caution must be exercised when centering the surgical field within the isocenter of the tracking volume. It is also important to minimize any equipment with ferromagnetic materials in the vicinity of the magnetic field generator.

Image-based instrument tracking is another alternative to using optical or magnetic spatial localization systems and is typically adopted when the procedure workflow may not easily allow the added technology. For example, procedures conducted under real-time cone-beam CT or X-ray fluoroscopy guidance cannot accommodate the use of a magnetic field generator in the field of view because it would interfere with the imaging acquisition. As an alternative, the instruments can be tracked directly in the X-ray images based on the unique 2D projection for a given pose of a 3D rigid body. Lang et al. demonstrated this approach for tracking a trans-esophageal echocardiography (TEE) probe for mitral valve (MV) repair and aortic valve implantation procedures [21,22]. Similarly, Novotny et al. proposed a GPU-based implementation of a rapid technique that detects the position and orientation of surgical instruments in the 3D real-time (26 fps) US images, based on passive markers attached to the instrument [23]. Both techniques require moderate instrumentation of the tools that are to be tracked using passive markers to allow their detection in the live image stream; they feature tracking accuracy of 2 mm or better, which is comparable to the accuracy achieved using electromagnetic tracking.

4.3 ACCURACY CONSIDERATIONS: CLINICAL REQUIREMENTS VERSUS ENGINEERING PERFORMANCE

While facilitating visualization and navigation under minimally invasive access and restricted direct vision, image guidance must at least maintain, and hopefully improve the outcome of the procedure. From a clinical perspective, procedure outcome could be interpreted as a binary assessment metric—pass/fail—in which a "pass" implies that safe therapy has been delivered, eliminating or improving the patient's condition and giving better quality of life. Although this may be regarded as the ultimate goal and evaluation metric of any procedure, from a quantitative perspective the outcome could be assessed based on a series of metrics based on targeting a specific location under specific time constraints. This leads to the ongoing debate of "How accurate is accurate enough?" typically accompanied by the common answer, "It depends…".

To address this question with a less generic answer, two other questions need to be answered: what is the tolerated uncertainty associated with the specific clinical procedure, and what is the uncertainty limit that could be delivered by the guidance system? The former is left to interpretation in the context of the procedure, patient, and physician. Examples include, but

are not limited to, the tissue margin required when excising a tumor from the surrounding soft tissue, the accuracy in targeting a specific site with a needle or catheter, the accuracy in positioning a valve in the outflow tract in a valve repair/replacement procedure, or the accuracy in positioning an implant in a specific bone site. The generic consensus of many physicians is that a sufficiently accurate navigation to within 5 mm of the desired location would be ideal because this approach would enable them to refine the final positioning based on the available real-time imaging and their clinical experience.

The latter question is based on metrics that can be evaluated in the laboratory or operating room, as the overall accuracy of the system cannot be better than its least accurate component. The image guidance workflow uses several processes and their associated uncertainties, all of which must be evaluated both independently, as well as part of the entire image guidance protocol, to determine their overall contribution to the ultimate navigation uncertainty.

Because interoperator variability associated with manual segmentation may be close to 5 mm, organ segmentation and modeling via semi- or fully automated approaches may lead to uncertainties on the order of several millimeters. Patient registration error, particularly for applications involving soft tissues, is also typically of the order of millimeters because a rigid registration may be used in lieu of a complex nonrigid algorithm simply because of time constraints. Last, surgical tracking yields errors on the order of 0.5 mm for optical tracking, and closer to 1.5–2 mm when using magnetic tracking. Several studies conducted in the laboratory under controlled conditions, and optimal image-to-subject registration, demonstrated that an overall targeting accuracy of around 1 mm could still be achieved using real-time intraoperative imaging, even where the images used for navigation purposes were subject to higher registration errors.

4.4 CLINICAL APPLICATIONS

4.4.1 Orthopedics

4.4.1.1 Pedicle Screw Instrumentation

Pedicle screw fixation for correction of spinal deformities has become the standard of care for stabilization of the thoracic and lumbar spine, where precise screw placement is essential to avoid injury to adjacent neural structures. However, the techniques currently available for planning such interventions are not optimal. Until recently, such procedures were

traditionally planned using 2D radiographs, an approach that has proved inadequate for precise planning due to the complex 3D anatomy of the spinal column and the close proximity of the nerve bundles, blood vessels, and viscera.

In conjunction with collaborating orthopedic surgeons, the research team at Mayo Clinic's Biomedical Imaging Resource has developed a clinician-friendly application that uses routine 3D CT or MRI data to generate detailed models and templates for better and more intuitive preoperative planning of pedicle screw instrumentation procedures. After importing the patient-specific MRI or CT dataset from an institutional picture archiving and communications system server, the planning process is conducted in two steps for each vertebral segment. First, each vertebra is reoriented such that the axial image plane is perpendicular to the central vertebral axis to correctly determine the true pedicle length and width at its narrowest point (i.e., screw length and diameter), together with the angle of approach (i.e., screw trajectory). In the second step, digital templates of pedicle screws are selected from a virtual pedicle screw template library that contains several standard instrumentation products, including different vendor and screw geometries. A pedicle screw type of desired size is selected and virtually "inserted" into the axial image. Optimal placement within the vertebra is achieved by interactively translating or rotating the implant in any of the three orthogonal views, while panning through the dataset for visual verification throughout the entire extent of the pedicle screw. Exact dimensions and angles of approach for each implanted screw are automatically determined upon final positioning and recorded in the planning report—the planning "recipe"—that provides a list of all instrumented vertebral segments, template screw type and manufacturer, screw dimensions (i.e., diameter and length), and the insertion trajectory defined according to the axial and sagittal angles measured relative to the vertebral axis. In addition to the implant list, the report also contains a collection of biplanar images showing each instrumented vertebral segment.

The final step of the preoperative plan is to produce a digital volume-rendered patient-specific 3D model of the spine along (Figure 4.1) with the virtual models of the inserted pedicle screws, which can be used with the generated report to prepare the instrumentation inventory for the operation. Moreover, the digital plan also can be easily translated into a full-size physical patient-specific model of the virtually instrumented spine using 3D printing or rapid prototyping.

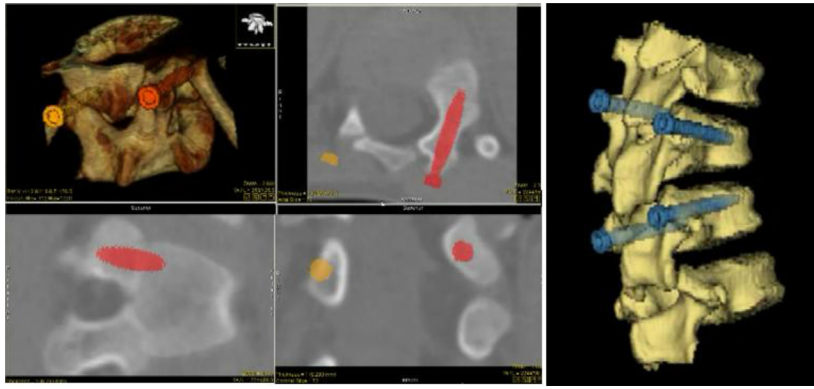

Figure 4.1 Snapshot of the spine surgery platform interface showing the interactive templating of the subject-specific computed tomography spine dataset visualized in the axial, coronal, and sagittal planes, accompanied by the resulting virtual model of the subject-specific instrumented spine segment.

4.4.1.2 Augmented Virtuality for Spine Needle Interventions

Spine needle interventions refer to the category of procedures involving the insertion of a needle into the spinal region. Among the common interventions are lumbar puncture (LP), epidural injection (EI), and facet joint injection. Although surgical targets are different in these procedures, these interventions share a common premise: the needle tip must be precisely placed within the target anatomy via a safe passage that avoids critical structures such as blood vessels during needle advancement.

All three of these interventions are performed for both diagnostic and therapeutic purposes. Common indications for LP include collection of cerebrospinal fluid for laboratory analysis (diagnostic), to relieving intracranial pressure (therapeutic), or to delivering injectant into the spinal canal. EI is most commonly used to deliver analgesic or local anesthetic agents, although it can also be used to administer diagnostic (e.g., radiocontrast) and other therapeutic agents. Facet joint injection is an interventional pain management tool for facet-related spinal pain. Often, facet joint syndrome cannot be diagnosed by medical imaging, so facet joint injection is used diagnostically to confirm a clinical suspicion of the facet joint syndrome. Therapeutically, it is used to deliver therapeutic agents to relieve the symptoms of facet joint syndrome.

Anatomically, target locations of LP and EI are very close to each other, so the surgical access or passage way for these two procedures is quite similar. The target site for LP is the subarachnoid space, sitting just below

the arachnoid membrane and dura mater in the spinal cord. In a living person, the arachnoid membrane and the dura mater exist in flush contact with each other from cerebrospinal fluid pressure: when a needle punctures the dura mater it also pierces the thinner arachnoid membrane. The target site for EI is the epidural space, sitting just outside the dura mater and surrounded by the osseous spinal canal. The epidural space is a *potential* space that, upon the injection of fluids, can be expanded to a *realized* space. Immediately surrounding the spinal canal is the ligamentum flavum that connects the laminae of adjacent vertebrae.

The facet joints are located between two vertebrae at the lateroposterior aspect of the spinal column. They are paired synovial joints formed by the articulation of the inferior articular processes of one vertebra with the superior articular processes of the vertebra below. Each joint is bordered medially and anteriorly by the ligamentum flavum and posteriorly by the multifidus muscle. The orientation of the facet joint varies across the column, thus understanding the exact anatomical orientation would facilitate the insertion of the needle.

The standard of care for both the LP and EI is the blind technique, relying solely on the tactile sensation and the experience of the medical practitioner. Once the correct intervertebral level is determined, and the appropriate interspace is located by palpation, the spinal needle is advanced incrementally through the tissue until there is a *give* tactile sensation indicating that the needle tip has passed the ligamentum flavum. The needle is further advanced until there is a *pop* sensation, which indicates the dura mater has been punctured and the needle tip is now located in the subarachnoid space. The success of LP is indicated by the appearance of cerebrospinal fluid, which slowly drains through the hollow needle due to the intracranial pressure.

For epidurals, the needle advancement is performed with the *loss of resistance* technique. Typically, a Tuohy needle with syringe (filled with air or saline) is used to avoid accidental puncture of the dura mater. Once the needle tip has entered the ligamentum flavum, the needle is advanced while the syringe is continuously being compressed. When the loss of resistance occurs, the air/saline is injected without resistance being felt when the tip of the epidural needle reaches the epidural space.

Facet joint injection is traditionally performed using a blind technique. As techniques evolve, the use of CT or fluoroscopy imaging is now preferred because imaging guidance allows more precise needle placement. Once the entry site is selected, the needle is advanced anteriorly until the

bone is reached. Once the needle tip enters the facet joint, a sensation of *give* is perceived. Repeated fluoroscopic imaging often is acquired to confirm the needle advancement and positioning.

Recently, several groups, including our own, have been investigating the use of US as a real-time guidance tool for spine needle interventions. US is particularly suited to visualizing superficial bony surfaces, allowing a preview of the anatomy and also to observe needle advancement in real time. The advantages offered by US-guided techniques include

- no harmful radiation to either the patient or the medical practitioner;
- reduced procedure time compared with CT- or fluoroscopy-guided techniques;
- ability to identify and hence avoid critical soft tissues such as vascular structures and dura;
- offers dynamic and real-time imaging, thus avoiding the need to continuously reposition the C-arm fluoroscope to obtain the optimal viewing angle; and
- lower cost and readier availability of US scanners compared with other imaging modalities.

These advantages are accompanied by the disadvantages of US-guided techniques:

- Long learning curve [24] for pattern recognition of the ultrasonographic appearance of the anatomical structures, and for probe handling and scanning skills to gain the ability to simultaneously manipulate the transducer and the insertion of the injection needle.
- The need for precise dexterity in aligning the needle to the US beam.
- The inability to resolve small anatomical features, either from the limitation of sonographic resolution or the operator's ability to recognize them.
- Difficulty in seeing deep tissues in certain patient populations.

The basic premise of our needle navigation system [25–27] is to provide a 3D visualization of the surgical scene to complement the streaming 2D US, thus assisting the operator's ability to understand and interpret the sono-anatomy. Our system comprises a standard clinical US scanner, equipped with a transducer appropriate for spinal imaging, and tracked with a 6 degrees-of-freedom MTS. A needle assembly, comprised of a standard hypodermic needle, syringe, and T-connector containing a tracking sensor, allows the needle to be tracked following calibration with a tracked calibration block. Guidance is provided to the anesthesiologist via a visualization/navigation system.

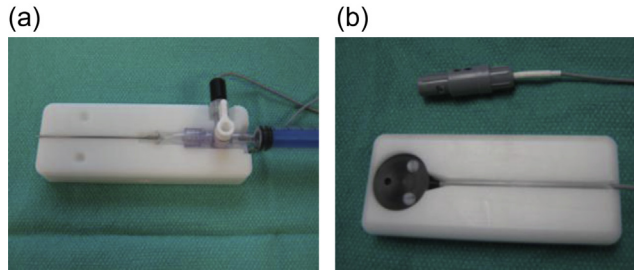

Figure 4.2 (a) Needle calibration block, containing the negative imprint of the needle assembly and (b) a 6 degrees-of-freedom magnetic tracking sensor.

In this configuration, all surgical instruments are spatially calibrated and tracked using the MTS, allowing the visualization software to render the 3D virtual representation of the surgical scene, together with the streaming US video (Figure 4.2). One critical design criterion in our approach was to use standard anesthesiology components as far as possible, leading to the design of a needle assembly with a calibration block instead of the more expensive, and disposable, commercial tracked needle.

The needle assembly comprises a hypodermic needle (needle tip type varies depending on the procedure performed) and a syringe, connected to a T-connector. A 6 degrees-of-freedom MTS sensor is attached to the assembly via the T-connector. In the clinical setting, the Luer taper and the MTS sensor cord would be enclosed by the sterile sheet before being connected to the T-connector. To calibrate for the orientation of the needle assembly with respect to the MTS sensor, we designed a custom calibration block, specific to the spine needle, comprising a 6 degrees-of-freedom MTS sensor, the negative imprint of the needle assembly, and a set of hemispherical divots at known locations. The hemispherical divots are used to register the negative imprint of the needle assembly to the attached MTS sensor. When the needle assembly is matched with the block, the spatial relationship between the two MTS sensors specifies the needle calibration (Figure 4.3).

The real-time tracking information is interpreted by the visualization software to render the surgical scene. When all the surgical instruments are properly calibrated and tracked, the rendition of the tracked needle should overlap with the needle reflection as seen in the US image. In this manner, the needle orientation can be directly visualized, improving the operator's needle handling dexterity (Figure 4.4).

Our needle guidance system has been evaluated [26,27] in a cadaveric study (Figure 4.5) to evaluate the system for facet joint injection. The

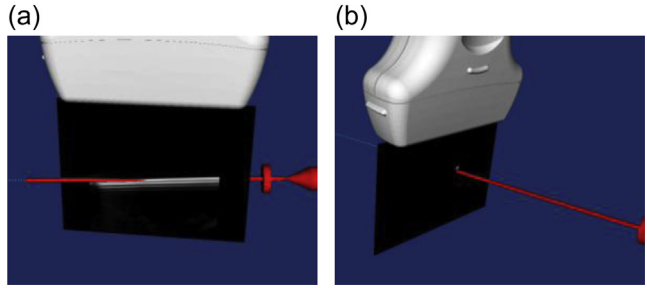

Figure 4.3 Two views (a), (b), depicting visualization of the relative pose between the tracked US probe and needle. When properly calibrated, the needle reflection in the sonographic image overlaps with the virtual representation of the needle.

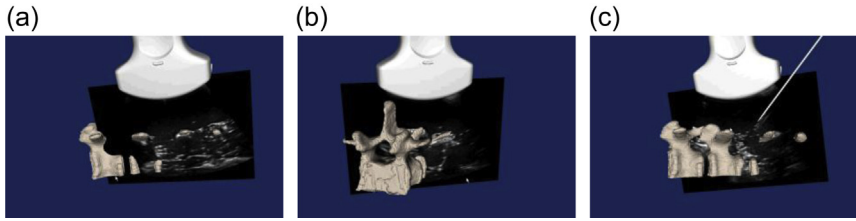

Figure 4.4 Augmented virtuality for spine needle guidance. Overlay of ultrasound video and osseous structures in (a) sagittal, (b) transverse view, and (c) needle advancement.

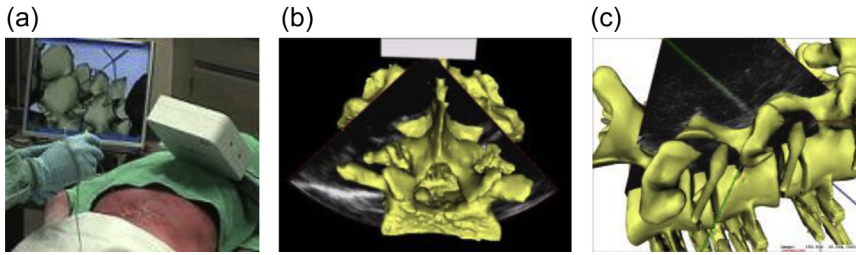

Figure 4.5 (a) Feasibility study of the needle guidance in cadaveric study, (b) augmented virtuality view of the spine anatomy with ultrasound overlay, and (c) enhancement of needle visualization in which the needle is highlighted in green.

objective of the evaluation was to quantify the accuracy of the guidance system for the delivery of injected anesthetic agent. In this case, an X-ray contrast agent was used instead of anesthetic. A CT scan of the lumbar vertebrae was acquired, allowing the virtual representation of the patient-specific osseous structures to be constructed. Specific anatomical landmarks

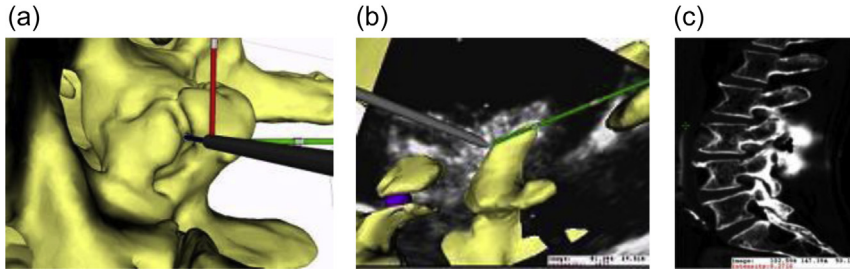

Figure 4.6 (a) Accurate placement of the needle tip in the facet joint, (b) real-time ultrasound is used to confirm needle placement, and (c) confirmation by radiopaque injectant in the X-ray image.

such as the tips of the spinous processes were identified in the CT scan, and subsequently in MTS-tracked US images, allowing the CT image to be registered to the patient using a paired-point registration algorithm [28].

After the registration of the surface model, four facet joints in the lumbar region were targeted, with needle guidance being facilitated by the navigation system, and the real-time US being used to confirm needle tip placement within the facet joint. To assess the efficacy of the system, radiopaque dye was injected into the facet joints, with subsequent CT images acquired to evaluate the distribution of the injected contrast agent. In this particular study (Figure 4.6), four facet injections were performed with only one procedure requiring two needle passes. Although the clinical adoption of the navigated/US-guided technique is in its early stage, our experience suggests that the use of tracking technology and 3D visualization system can be a useful adjunct for spine needle interventions.

4.4.2 Abdominal Laparoscopic Applications

Many abdominal procedures can be performed using endoscopy as a viable alternative to open surgery. In such minimally invasive approaches, surgical instruments gain surgical access through small ports on the patient's skin and imaging is provided by a video camera (laparoscope/endoscope) as a substitute for direct vision, thus providing the superficial view of the surgical scene. Often, US is used to depict subcutaneous structures beyond the organ wall. In a typical setup, the US and endoscopic video streams are displayed on two separate monitors located close to the operating room table. The surgeons therefore must perform spatial reasoning to mentally map the US image into the video. Furthermore, the 2D nature of these images results in decreased depth perception.

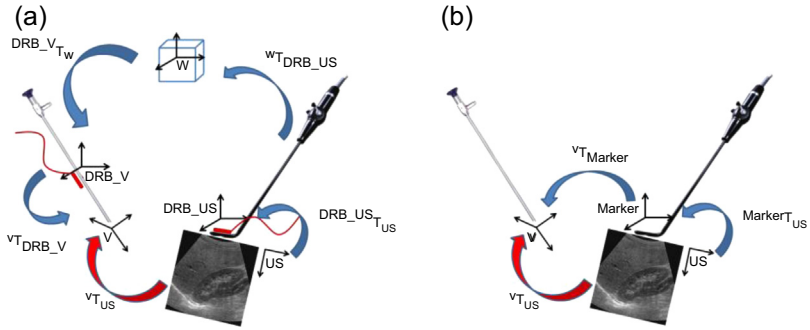

Figure 4.7 Schematic of navigated endoscopic tracking using (a) extrinsic and (b) intrinsic (vision) tracking systems. The ability to fuse ultrasound (US) into video depends on the accurate estimation of the transition $^{V}T_{US}$. The local coordinate system of the extrinsic tracking system (often magnetic) is used as the world coordinate system (W), where the WTDRB denotes the tracker transformations. DRB_USTUS denotes the US calibration matrix and VTDRB_V denotes the camera calibration.

Navigated endoscopy [29] incorporates a spatial tracking device to infer the pose of the US probe relative to the camera, allowing the US images to be registered and fused with the video. Although most research groups use an *extrinsic* tracking device (such as photo-acoustic [30], magnetic [31], or robotic [32]), we have developed navigated endoscopy systems using either extrinsic (magnetic) [31] or the endoscopic camera itself as an *intrinsic* tracking device [33] (Figure 4.7). Compared with an extrinsic tracking device, such an approach does not incur additional costs, instruments require no additional sterilization, and it does not impact surgical workflow. Vision-based tracking [34] must, however, overcome the limitation of endoscopic lighting conditions, be sufficiently robust to work when occluded by surgical tools, and satisfy accuracy and frame rate requirements.

The ability to fuse US image with laparoscopic video is achieved by spatially tracking the surgical instruments and calibrating the US probe and video camera. A comprehensive review of US calibration can be found in Ref. [35]. Video camera calibration is comprised of two distinct calibration processes. First, a 3D optical axis needs to be defined based on the geometry of the camera lens; this can be achieved using the standard technique described in Ref. [36]. Second, the spatial relationship of this optical axis needs to be calibrated against the extrinsic tracking system, which can be performed using the "hand-eye" calibration technique described in Ref. [37]. When both the US and the video camera are properly calibrated, the

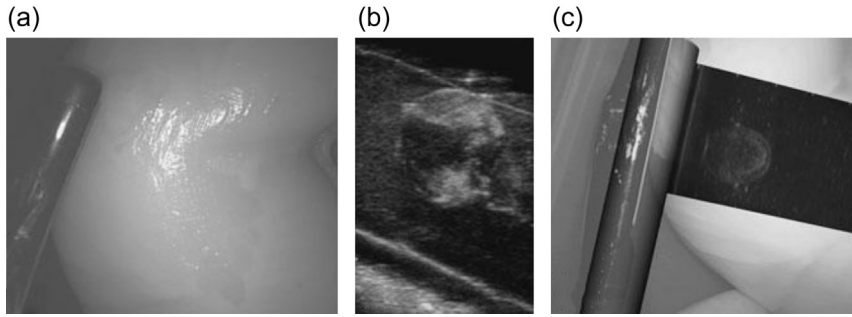

Figure 4.8 (a, b) Separate video and ultrasound (US) images, with the US transducer visible in the video stream and (c) fused US image and video showing a tumor within a phantom.

transformation chain is closed (see Figure 4.7(a)), allowing the US image to be related to the optics axis to achieve image fusion.

Image fusion can be achieved when the transformation ${}^{V}T_{US}$, as shown in Figure 4.7, can be reliably estimated. Using an extrinsic tracking device, ${}^{V}T_{US}$ can be obtained from a series of transformation chains, involving the tracked poses of each surgical instruments as well as the respective calibrations. Using this principle, we have developed an MTS-based navigated endoscopic system for partial nephrectomy (Figure 4.8) demonstrating in a laboratory setting that the system was sufficiently accurate for clinical use, while reducing surgical planning time [31].

An intrinsic tracking system using the laparoscopic camera to perform spatial measurement [34] does not share the same limitation as those using an extrinsic tracking device, but often suffers from issues involving accuracy, robustness, and the need to modify standard surgical instruments. To address some of these issues, we proposed a system that uses a standard monocular endoscopic video camera, capable of tracking a nonplanar pattern, and is robust to partial visual occlusion [33].

Similar to other vision-based tracking systems [34], our system relies on the visual tracking of a pattern composed of a set of features arranged in a known geometry. An example of a pattern would be a checkerboard with a known number of rows and columns, where the intersection of black and white squares serves as a feature. The particularity of our approach is that we do not require the detection of the whole pattern. Instead, we use a Kalman-filter based approach [38] to simultaneously perform

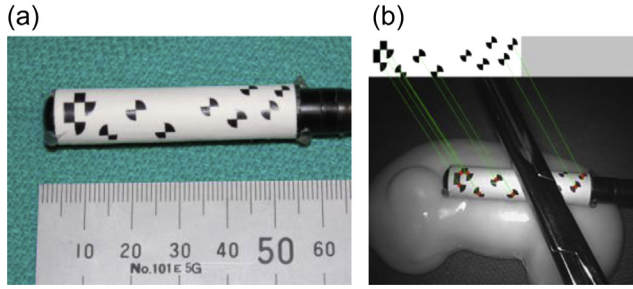

Figure 4.9 (a) Three-dimensional pattern attached to the back surface of the tubular ultrasound transducer. The visual tracking algorithm works in the presence of occlusion and endoscopic lighting variations (b).

feature correspondence and *pose-estimation*, allowing our approach to reliably estimate the pose of endoscope using a minimum of four features out of the full pattern. Furthermore, our approach does not require the pattern to be planar: it could be a 3D pattern etched on the back of a curved US probe. In this manner, our approach is robust to visual occlusion when a surgical instrument partially blocks the view of the camera, and works under endoscopic lighting condition where the strong specular lighting condition often make features on a pattern hard to detect.

We demonstrated our image fusion system with intrinsic tracking system using the following example. A 3D pattern comprising 11 checkerboard features was rigidly attached to the back of a laparoscopic US probe (Figures 4.9 and 4.10).

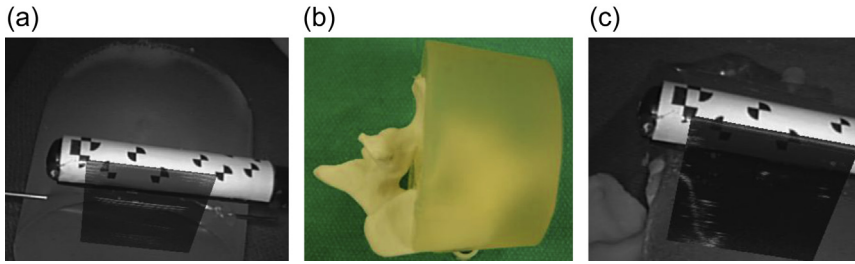

Figure 4.10 Visual tracking using monocular camera with ultrasound (US) overlay. (a) A metallic needle is threaded to a piece of US-compatible solid: the reflection of the needle in US and the needle in the video image form a straight line. (b) A spine vertebra is semisubmerged into an US-compatible solid. (c) The reflection of the anterior process of the vertebrae in US forms a continuous outline with the camera image.

Under endoscopic lighting condition and with partial occlusion from another surgical instrument, our visual tracker was able to establish feature correspondence and hence recover the pose of the 3D pattern (Figure 4.9(b)).

Image fusion between US and video streams can be achieved once the laparoscopic US is calibrated against the 3D pattern. Figure 4.10 depicts the capability of our visual tracker: a foreign object (metallic needle in Figure 4.10(a) and spine vertebrae in Figure 4.10(b) and (c)) is submerged into an US medium; the image overlay of the US to the video shows a continuous and seamless outline of the foreign object between two image modalities. Using better computational power and a more efficient software implementation, we believe that our intrinsic tracker could achieve the speed and accuracy comparable to an extrinsic tracking system, making it a viable alternative for clinical use.

4.4.3 Neurosurgical Applications

4.4.3.1 Stereotactic Neurosurgery

Image-guided neurosurgery is in regular use in the operating room, with important applications in the surgical treatment of Parkinson disease (PD), essential tremor, and chronic pain via minimally invasive methods. These procedures involve the creation of lesions by resection or thermal ablation or by placing chronic stimulators in precise locations relative to certain electrophysiologically defined regions in the deep brain. The location of the targets must first be identified on preoperative MRI or CT scans, and then the targets refined based upon electrophysiological probing of the target site. Because target regions are not well visualized on the preoperative images, standard atlases are often registered to the patient as a surrogate to define the approximate location of the target [39] or by using digitized versions of these standard atlases [40].

The use of brain atlases in neuroscience has been an active research area for many years [41], and the integration of digitized atlases into planning systems to facilitate functional neurosurgery has resulted in a number of independent efforts [42–45]; commercially available surgical planning systems also have incorporated anatomical atlas-based planning modules [46]. Registration of the atlas to the patient is typically achieved using linear scaling techniques based primarily on the length of the anterior commissural–posterior commissural line and the width of the third ventricle [47]. Some research-oriented systems also incorporate automatic nonlinear registration algorithms for this task [45,48–50]. When various views of a digitized atlas

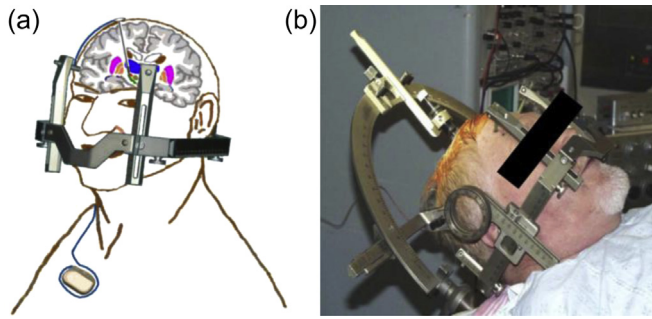

Figure 4.11 (a) Stereotactic frame mounted on patient (b) with isocentric arc attached to guide probe to target during surgery.

are displayed within a surgical planning system, virtual probe trajectories to an atlas-predicted target may be modeled prior to surgery. The stereotactic coordinates of the target can then be transferred to a stereotactic guidance system displayed to the surgeon. Because the purely anatomical approaches do not consider the electrophysiological characteristics of the targets directly, these may be augmented by electrophysiological atlases [43,49,50] giving the surgeon a probabilistic target region based on pooled electrophysiological data from a cohort of previous patients.

In most cases, a stereotactic frame containing coordinate reference markings, along with an arc that can hold an instrument, is used to direct a probe to the specific target. During imaging, the frame is fitted with an acrylic box containing N-shaped fiducial markers that can be identified in either MRI or CT imaging, so they are visible on the volumetric images of the patient. Registration of the image-based markers with those of the frame provides a method of registering the coordinate system of the image to that of the frame. Following registration, the voxels identified in the 3D images can be uniquely related to frame coordinates. More recently, similar targeting has been achieved using "frameless stereotactic" techniques, whereby the preoperative images are registered to the patient via scalp-mounted markers, and electrodes are introduced into the patient's brain via a skull-mounted device that can advance an electrode to a specific depth [51]. The configuration of the frame is illustrated in Figure 4.11.

4.4.3.2 Image-Based Planning for Epilepsy

Unlike PD, epilepsy can arise from foci anywhere in the brain, but is often confined to regions within the temporal lobes. Delineation of the epileptogenic zone, however, can be very difficult, especially in patients who do not present any apparent anatomical lesions on conventional MRI.

Although classical late-stage hippocampal sclerosis is readily identified, early or atypical hippocampal sclerosis patients have distinct pathology and surgical outcomes, but the two types are indistinguishable using conventional imaging. Furthermore, subtle extrahippocampal pathology, such as cortical dysplasia, may be missed altogether in the resection area because of the lack of sensitivity in imaging. Specificity in imaging is also lacking, and recent histopathological studies have shown that blurring of the gray–white boundary, once thought to be epileptogenic, is more likely related to dysmyelination [52]. These findings have motivated the development of more sensitive and specific imaging and analysis techniques to better delineate target regions for more effective surgery. Accordingly, there is increasing interest in performing epilepsy imaging using multiparametric imaging sequences that produce maps of the underlying T1 and T2 relaxation parameters as well as images that depict quantitative diffusion parameters, rather than simply looking at T1- and T2-weighted images. As a result, recent research has focused on quantifying the differences seen in these quantitative images between epilepsy patients and healthy individuals [53]. This work demonstrated quite clearly that there is information in MRI scans, which when analyzed quantitatively, can serve as specific markers of pathology in the brain. The long-term goal of such work is to validate the MRI signals against histological samples acquired from resected tissue and to use these multiparametric images as predictors of pathology in the operating room. This information may then be presented to the surgeon via a standard image-guided neurosurgery platform that registers the patient to preoperative images, and tools tracked by either optical or magnetic means

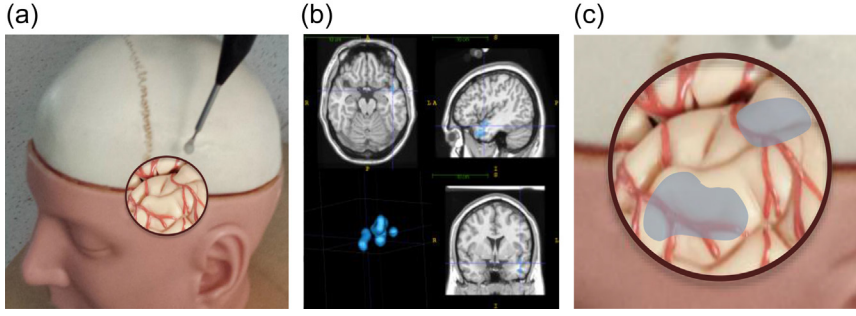

Figure 4.12 Illustration of potential display of information in the operating room. (a) Surgical field of view of patient. (b) Conventional visualization with overlaid pathology regions. (c) Surface-based visualization, with video feed and overlaid pathology regions displayed in blue.

would be represented accurately on a video display with respect to the "pathology data" rendered on the display screen (Figure 4.12).

More recent proposals for the treatment of epilepsy have much in common with the procedures for PD described previously. Rather than resect the region of the brain deemed to contain the focus, the approach is to inject small electrical currents into the brain tissue to disrupt the electrical pathways responsible for propagating the seizures [54,55]. Typical targets may include ones similar to those used for PD therapy (regions of the thalamus or subthalamic nucleus for example) or regions in the temporal lobe or cerebellum. Precise mechanisms are not understood, but it is believed that the injected currents act either to gate the pathways of the epileptic discharges or to directly inhibit the epileptic focus itself, if that is where the electrode is placed. An even more recent approach identifies a target in a manner similar to the placement of depth electrodes, but this time using an optical fiber capable of delivering heat energy to the target via a high-intensity laser [56].

4.4.3.3 Image-Guided Tumor Removal

Although the majority of tumor surgery is currently performed using a craniotomy, possibly with some guidance from a standard image-guidance platform such as the Medtronic Stealth Station® or Brainlab's iPlan®, there is growing interest in performing such procedures in a minimally invasive manner. For example, by instruments such as the NICO© "Brain-path" device that is inserted through a burr hole in the skull and into a sulcus adjacent to the tissue to be resected. By careful planning based on preoperative images that show anatomy, vessels, and white-matter tracts, the tumor can be safely approached via the cannula, ensuring that critical tissue remains intact. Because the tumor is approached via the sulcal wall, collateral damage to healthy brain tissue is minimized (Figure 4.13).

4.4.4 Cardiac Applications

4.4.4.1 Transapical Aortic Valve Replacement

The standard of care for patients with severe aortic valve stenosis is open-heart surgery. The patient is placed on cardiopulmonary bypass, allowing the surgeon direct tactile and visual access to the surgical target site. However, because of trauma associated with cardiopulmonary bypass and aortic cross-clamping, up to one-third of all patients are deemed inoperable because of comorbidities such as pervious cardiac surgeries, chronic lung disease, and renal failure [57]. In response to this problem, beating-heart techniques are being developed. Stent-based beating-heart aortic valve

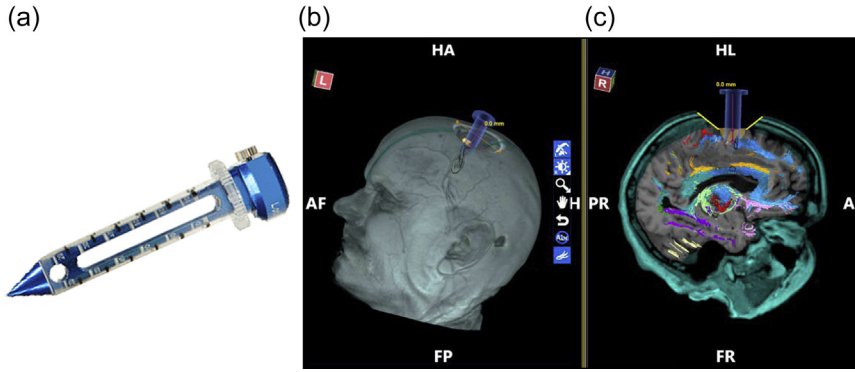

Figure 4.13 (a) NICO Brain-path® instrument for minimally invasive access to brain tissue. The pointed instrument, surrounded by a plastic cannula, is inserted into the sulcus close to the tumor to be removed. Once in place, the central core is removed, and the tumor is aspirated through the cannula that remains in place. (b) Synaptive's BrightMatter® planning software maneuvering the cannula relative to a tumor. (c) The BrightMatter platform showing pathway to tumor in relation to the patient's (magnetic resonance imaging) brain and nerve bundles.

replacement was first performed in humans in 2002, with more than 50,000 cases performed in more than 40 countries since then [58].

Access to the aortic valve is achieved either transfemorally, via apical entry through the left ventricle (LV), or directly through incision into the descending aorta. The latter two techniques require a minithoracotomy for access, but provide more direct control of the delivery tool. Stents are either made from a shape-memory alloy or use an inflatable balloon for deployment. Since their inception, a wide variety of devices are currently in the market (Figure 4.14).

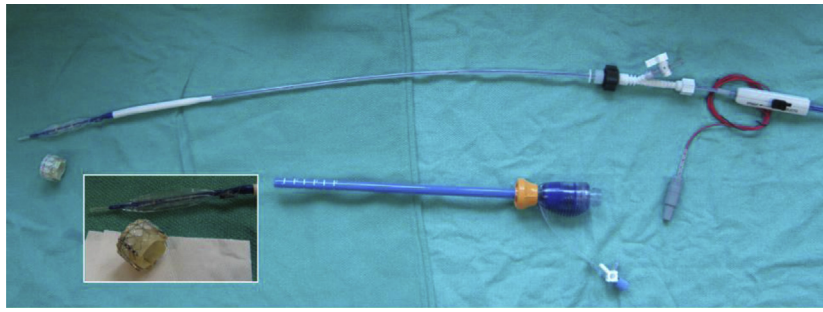

Figure 4.14 Portions of the Edwards' SAPIEN transaortic valve replacement system [59]. Bottom center: the introducer used to gain safe access to the apex of the left ventricle. Insert: close-up of the valve stent and inflatable balloon. Top: the primary introducer device, retrofitted with a magnetic sensor (red cable).

Because these procedures are performed while the heart is still beating, surgeons rely on image guidance to safely and effectively perform the therapy. While US (TEE) is ubiquitous in cardiac interventions, it is inadequate as a guidance modality primarily because of shadow artifacts from the valve stent occluding crucial anatomy (valve nadir and commissures as well as coronary ostia). Consequently, transapical aortic valve replacement standard of care relies primarily on fluoroscopy, the other imaging modality ubiquitous in cardiac interventions. Image guidance is crucial to ensure proper stent placement; a stent deployed too far inside the LV may embolize, whereas a stent deployed too far into the aorta may occlude the coronary ostia. Further, if the stent is not coaxial with the native valve there is a significant risk of paravalvular leak.

Commercial systems such as Siemens DynaCT [60] use intraoperative C-arm cone-beam reconstructions to facilitate optimal valve orientation and positioning during real-time fluoroscopic imaging, while the Philips HeartNavigator system [61] integrates fluoroscopy with echocardiography. Recently, in an attempt to eliminate the need for contrast agents as well as radiation dose to both patient and clinician, researchers have been developing techniques for performing transapical aortic valve replacement using TEE augmented with information from magnetically tracked tools [62,63]. In this technique, magnetic sensors are integrated into or onto both the TEE probe and the catheter delivery tool. The US image data are then augmented with virtual models indicating the location of relevant tools and patient anatomy (ostia, valve nadir, or commissures, Figure 4.15).

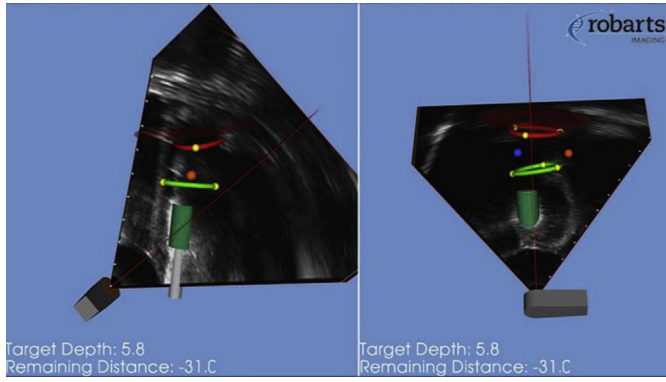

Figure 4.15 Mixed reality guidance for transcatheter aortic valve replacement: real-time ultrasound data from the transesophageal echocardiography (TEE) probe is integrated with a model of the tracked stent (green) and relevant anatomy is defined from the tracked TEE (red/green splines define valve nadir/commissures, blue/orange spheres mark coronary ostia locations).

Segmentations of the aortic root derived from preoperative CT can be registered into the scene if required.

4.4.4.2 MV Repair

Just as many patients are judged high risk for open-heart aortic valve repair/replacement, many patients with functional or degenerative MV disease are unable to receive standard-of-care (on-pump open-heart surgery) treatment. Although MV replacement/implantation devices are widely under development, current options for high-risk patients are limited to MV repair techniques, such as the transfemoral MitraClip (Abbot Vascular Inc.) and the LV apical access NeoChord (NeoChord Inc.).

Unlike aortic valve replacement, fluoroscopy is of limited use for guiding MV repairs given the excessive amount of contrast agent required to identify the MV anatomy using this modality. Consequently, beating heart MV repair procedures rely primarily on 2D and 3D TEE US guidance. In the case of the NeoChord procedure, 2D and 2D biplane TEE are used to navigate from the LV apical entry point to the region of the MV. Unfortunately, the limited field of view and lower resolution of 3D TEE makes it unsuitable for this stage of the procedure. However, once the device is in the target region, 3D TEE is used to identify the exact target position on the MV leaflet. The surgeon then returns to 2D TEE for the actual grasping of the MV leaflet. In the context of image guidance challenges, the process of final tool positioning and leaflet grasping are well handled by 3D and 2D TEE, respectively.

However, the process of safely navigating the tool from its entry point at the apex of the LV to a point between the two rapidly moving MV leaflets is quite challenging. To assist with this task, the NeoNav guidance system (www.neochord.com/index.php/neonav) uses magnetic tracking technology to track and visually integrate real-time US with tool and anatomic geometric models (Figure 4.16). This system has demonstrated significant improvement in the safety and speed of the procedure [64].

4.4.4.3 Left Atrial Ablation Guidance and Monitoring

The prototype system for advanced visualization for image-guided left atrial ablation therapy developed at the Biomedical Imaging Resource (Mayo Clinic, Rochester, MN, USA) [65] uses an architecture that allows the integration of pre- and intraoperative imaging, catheter localization, and electrophysiology information into a single user interface. Although sufficiently general to be used in various catheter procedures, the system has

Figure 4.16 Right, animal trial of augmented ultrasound guidance for beating-heart mitral valve repair. Left top, the NeoChord tool, retrofitted with magnetic sensors resting on the NDI Aurora Tabletop tracker. Left bottom, tool tip path data with transesophageal echocardiography (TEE) only and augmented TEE compared (green ring represents mitral valve annular ring).

been primarily tested and evaluated for the treatment of left atrial fibrillation.

The system interfaces to a commercial cardiac mapping system that relays catheter position and orientation information, whereas the user interface displays a surface-rendered, patient-specific model of the left atrium and associated pulmonary veins. These are segmented from a pre-operative contrast-enhanced CT scan, along with a point cloud sampled intraoperatively from the endocardial left atrial surface using the tracked catheter. The model-to-patient registration is initialized using a set of anatomical landmarks and continuously updated during the procedure as additional endocardial points are sampled within the left atrium [66]. These data are further augmented with real-time US images acquired using a tracked intracardiac echocardiography probe, allowing the display of the acquired US imaged in their correct pose relative to the preoperative left atrial model registered to the patient (Figure 4.17).

Once on target, radiofrequency energy is delivered to the tissue under lesion visualization information provided by an integrated image-based ablation model that predicts tissue temperature distribution and lesion quality (reversible vs irreversible tissue damage) based on the delivered energy and tissue properties [67]. Ongoing developments currently focus on the real-time lesion visualization in response to the radiofrequency energy delivery, which is provided to the clinician in the form of local temperature maps and lesion geometry and characterization superimposed onto the patient-specific left atrial model.

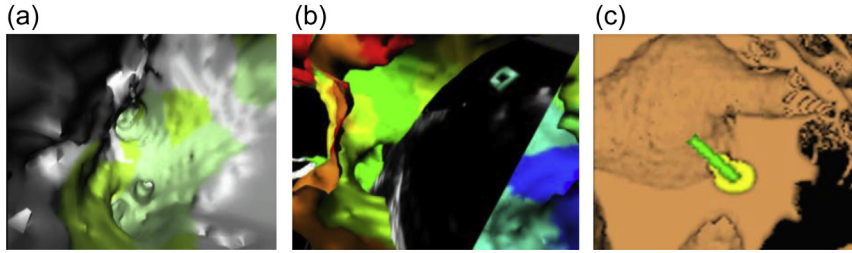

Figure 4.17 Example of electro-anatomical model of the left atrium showing (a) the activation times at one of the pulmonary vein bifurcations, also complemented (b) with real-time ultrasound imaging. (c) Volume-rendered representation of the ablation lesion modeled via the image-based thermal model superimposed onto the preoperative volume-rendered anatomy.

4.5 LIMITATIONS, CONSTRAINTS, AND CHALLENGES

4.5.1 Design Constraints and Criteria

The principle of "form follows function" is fundamental in the design of medical devices for IGI. Numerous factors impact tool design depending on the circumstances in which the device is expected to function. Imaging modalities, target tissue access, therapy task, tracking technologies, operating room footprint, and workflow all play a role in the final design of any tool.

Every imaging modality imposes some form of constraint on materials and tool design. Metals and other materials with high electron densities can cause spoke artifacts and shadowing in CT, materials with poor echogenicity can cause artifacts such as shadowing in US, and ferromagnetic materials cannot be used at all in MRI. These problems can be compounded for multimodality IGI and applications using image-based tracking technology.

Most IGI applications require some form of tracking technology to register surgical tools into a guidance framework. A wide range of tracking technologies exists, and which is optimal for a given application depends on the accuracy required and the specific nature of the intervention. For example, in the case of intracardiac IGI as described previously, rigid tools are rarely possible, thus making line-of-sight optical tracking impossible. In consequence, MTS or some form of image-based tracking is needed, thus affecting tool design. In contrast to intracardiac applications, orthopedic applications typically involve rigid targets and rigid tools, making optical tracking appropriate. Robotic, optical, and magnetic tracking technologies offer high degrees of accuracy and simplicity of implementation, but they also increase the overall operating room footprint of an IGI system, requiring integration of fiducials or sensors into devices. If geometric

designs of the tool can be appropriately identified in the imaging modalities used, it may be possible to track devices directly from raw image data. However, this approach tends to be computationally expensive and can be difficult to implement in a sufficiently robust manner for IGI.

Given the range of constraints on device design, it is important to carefully define both the task a device must perform and its place within a surgical workflow when preparing design specifications for any tool. A clear and comprehensive understanding of surgical workflow, imaging, and tracking requirements is necessary prior to preparing any design specifications.

4.5.2 Clinical Implementation Limitations

In developing new image guidance approaches, clinical applications for which there already exist a standard practice and workflow tend to have a higher level of inertia. In the absence of a pressing medical or financial need, the medical community may be slow to adopt new and potentially advantageous technology simply because current standard of care is "good enough." In contrast, new surgical techniques for which there are image guidance challenges can provide excellent opportunities for integrating new image guidance technologies at an early stage. Regardless, "early adopters" within the clinical community are usually critical to the acceptance of new surgical techniques. Forging close, reciprocal relationships with clinicians not only improves the utility of new medical devices, but also encourages adoption into the wider medical community.

4.5.3 Regulatory Constraints

The topic of regulatory constraints could easily fill a book in its own right, with different countries and jurisdictions having different requirements. Not only do regulatory requirements vary geographically but they also vary with different surgical applications. In broad terms, the complexity of regulatory requirements increases dramatically as one progresses from proof-of-concept work in a laboratory setting to full commercial development of a device for use in humans.

4.6 SUMMARY AND FUTURE DIRECTIONS

IGI technology continues to develop, stimulated both by improvements in computing and image-processing capabilities, hardware to support tracking and visualization, and the increasing number of surgeons who are willing to embrace nontraditional technologies. Although IGI techniques are well

established in the neurosurgical and orthopedic fields, applications in other areas of the body remain mostly in prototype form, with only limited clinical exposure.

As the push toward minimally invasive interventions continues, image guidance will be increasingly used to improve the precision and outcome of surgical procedures. However, wider clinical acceptance of this technology only will occur through close partnerships between scientists and surgeons, compelling studies that conclusively demonstrate major benefits in terms of patient outcome and cost, and a commitment from the surgical device industry to support these concepts.

REFERENCES

[1] Galloway R, Peters TM. Overview and history of image-guided interventions. In: Peters TM, Cleary K, editors. Image-guided interventions: technology and applications; 2008. p. 1–21. New York: Springer.
[2] Ettinger GL, Leventon ME, Grimson WEL, Kikinis R, Gugino L, Cote W, et al. Experimentation with a transcranial magnetic stimulation system for functional brain mapping. Med Image Anal 1998;2:477–86.
[3] Botden SM, Jakimowicz JJ. What is going on in augmented reality simulation in laparoscopic surgery? Surg Endosc 2009;23:1693–700.
[4] Feifer A, Delisle J, Anidjar M. Hybrid augmented reality simulator: preliminary construct validation of laparoscopic smoothness in a urology residency program. J Urol 2008;180:1455–9.
[5] Kerner KF, Imielinska C, Rolland J, Tang H. Augmented reality for teaching endotracheal intubation: MR imaging to create anatomically correct models. Proc Annu AMIA Symp 2003;2003:888–9.
[6] Rolland JP, Wright DL, Kancherla AR. Towards a novel augmented-reality tool to visualize dynamic 3-D anatomy. Stud Health Technol Inf 1997;39:337–48.
[7] Kaufman S, Poupyrev I, Miller E, Billinghurst M, Oppenheimer P, Weghorst S. New interface metaphors for complex information space visualization: an ECG monitor object prototype. Stud Health Technol Inform 1997;39:131–40.
[8] Koehring A, Foo JL, Miyano G, Lobe T, Winer EA. Framework for interactive visualization of digital medical images. J Laparoendosc Adv S 2008;18:697–706.
[9] Lovo EE, Quintana JC, Puebla MC, Torrealba G, Santos JL, Lira IH, et al. A novel, inexpensive method of image coregistration for applications in image-guided surgery using augmented reality. Neurosurgery 2007;60:366–71.
[10] Nakamoto M, Nakada K, Sato Y, Konishi K, Hashizume M, Tamura S. Intraoperative magnetic tracker calibration using a magneto-optic hybrid tracker for 3-D ultrasound-based navigation in laparoscopic surgery. IEEE Trans Med Imaging 2008;27:255–70.
[11] Teber D, Guven S, Simpfend T, Baumhauer M, Gven EO, Yencilek F, et al. Augmented reality: a new tool to improve surgical accuracy during laparoscopic partial nephrectomy? Preliminary in vitro and in vivo results. Eur Urol 2009;56:332–8.
[12] Vogt S, Khamene A, Niemann H, Sauer F. An AR system with intuitive user interface for manipulation and visualization of 3D medical data. In Proc. MMVR. Stud Health Technol Inf 2004;98:397–403.
[13] Vosburgh KG, San José Estépar R. Natural orifice transluminal endoscopic surgery (NOTES): an opportunity for augmented reality guidance. In Proc. MMVR. Stud Health Technol Inf 2007;125:485–90.

[14] Linte CA, Davenport KP, Cleary K, Peters C, Vosburgh KG, Navab N, et al. On mixed reality environments for minimally invasive therapy guidance: systems architecture, successes and challenges in their implementation from laboratory to clinic. Comput Imaging Graph 2013b;37:83–97.
[15] Hounsfield GN. Computerized transverse axial scanning (tomography). 1. Description of system. Br J Radiol 1973;46:1016–22.
[16] Bronskill M, Sprawls P. The physics of MRI. In: Proc. AAPM summer school; 1993.
[17] Fahrig R, Holdsworth DW. Three-Dimensional computed tomographic reconstruction using a c-arm mounted XRII: image-based correction of gantry motion nonidealities. Med Phys 2000;27:30–8.
[18] Jaffray DA, Siewerdsen JN, Wong JW, Martinez AA. Flat-panel cone-beam computed tomography for image-guided radiation therapy. Int J Radiat Oncol Biol Phys 2002;53:1337–49.
[19] Siewerdsen JH, Moseley DJ, Burch S, Bisland SK, Jaffray DA, Bogaards A, et al. Volume CT with a flat-panel detector on a mobile, isocentric c-arm: pre-clinical investigation in guidance of minimally invasive surgery. Med Phys 2005;32:241–54.
[20] Stephenson SK, Chang EK, Marks LS. Screening and detection advances in magnetic resonance image-guided prostate biopsy. Urol Clin North Am 2014;41(2):315–26.
[21] Lang P, Rajchl M, Currie ME, Daly RC, Kiaii B. Augmented reality image guidance improves navigation for beating heart mitral valve repair. Innovations (Phila) 2012a; 7(4):274–81.
[22] Lang P, Seslija P, Chu MWA, Bainbridge D, Guiraudon GM, Jones DL, et al. US-fluoroscopy registration for transcatheter aortic valve implantation. IEEE Trans Biomed Eng 2012b;59:1444–53.
[23] Novotny PM, Stoll JA, Vasilyev NV, del Nido PJ, Dupont PE, Zickler TE, et al. GPU based real-time instrument tracking with three-dimensional ultrasound. Med Image Anal 2007;11(5):458–64.
[24] Awad I, Chan V. Ultrasound imaging of peripheral nerves: a need for a new trend. Region Anesth Pain Med 2005;30(4):321–3.
[25] Chen ECS, Ameri G, Li H, Sondekoppam RV, Ganapathy S, Peters TM. Navigated simulator for spinal needle interventions. Med Meets Virtual Real 2014;21(196):56–60.
[26] Moore J, Clarke C, Bainbridge D, Wedlake C, Wiles A, Pace D, et al. Image guidance for spinal facet injections using tracked ultrasound. Med Image Comput Comput Assist Interv 2009;5761:516–23.
[27] Clarke C, Moore J, Wedlake C, Lee D, Ganapathy S, Salbalbal M, Wilson T, Peters T, Bainbridge D. Virtual reality imaging with real-time ultrasound guidance for facet joint injection: a proof of concept. Anesth Analg 2010;110(5):1461–3.
[28] Horn BKP. Closed-form solution of absolute orientation using unit quaternions. J Opt Soc Am A 1987;4(4):629–42.
[29] Langø T, Vijayan S, Rethy A, Våpenstad C, Solberg OV, Mårvik R, et al. Navigated laparoscopic ultrasound in abdominal soft tissue surgery: technological overview and perspectives. Int J Comput Assist Radiol Surg 2012;7(4):585–99.
[30] Cheng A, Kang JU, Taylor RH, Boctor EM. Direct 3D ultrasound to video registration using photoacoustic effect. Med Image Comput Comput Assist Interv 2012;7511:552–9.
[31] Cheung C, Wedlake C, Moore J, Pautler SE, Peters TM. Fused video and ultrasound images for minimally invasive partial nephrectomy: a phantom study. Med Image Comput Comput Assist Interv 2010;6363:408–15.
[32] Leven J, Burschka D, Kumar R, Zhang G, Blumenkranz S, Dai XD, et al. DaVinci canvas: a telerobotic surgical system with integrated, robot-assisted, laparoscopic ultrasound capability. Med Image Comput Comput Assist Interv 2005;3749:811–81.

[33] Jayarathne UL, Mcleod AJ, Peters TM, Chen ECS. Robust intraoperative US probe tracking using a monocular endoscopic camera. Med Image Comput Comput Assisted Interv 2013;8151:363–70.
[34] Pratt P, Di Marco A, Payne C, Darzi A, Yang G-Z. Intraoperative ultrasound guidance for transanal endoscopic microsurgery. Med Image Comput Comput Assist Interv 2012;7510:463–70.
[35] Mercier L, Langø T, Lindseth F, Collins DL. A review of calibration techniques for freehand 3-D ultrasound systems. Ultrasound Med Biol 2005;31(2):143–65.
[36] Bradski G, Kaehler A. Learning Opencv. 1st ed. O'Reilly Media, Inc. 2008.
[37] Chen ECS, Sarkar K, Baxter JSH, Moore J, Wedlake C, Peters TM. An augmented reality platform for planning of minimally invasive cardiac surgeries. In: Holmes III DR, Wong KH, editors. Proc. SPIE, vol. 8316; 2012. 831617–831617–10.
[38] Moreno-Noguer F, Lepetit V, Fua P. Pose priors for simultaneously solving alignment and correspondence. Comput Vision–ECCV 2008;5303:405–18.
[39] Schaltenbrand G, Wahren W. Atlas for stereotaxy of the human brain with guide to the Atlas for stereotaxy of the human brain. Stuttgart: Thieme; 1977.
[40] Nowinski WL, Yang GL, Yeo TT. Computer-aided stereotactic functional neurosurgery enhanced by the use of the multiple brain atlas database. IEEE Trans Med Imaging 2000;19(1):62–9.
[41] Thompson PM, Woods RP, Mega MS, Toga AW. Mathematical/computational challenges in creating deformable and probabilistic atlases of the human brain. Nature 2000;404(6774):190–3.
[42] Dawant BM, Hartmann SL, Pan S, Gadamsetty S. Brain atlas deformation in the presence of small and large space-occupying tumors. Brain atlas deformation in the presence of small and large space-occupying tumors. Comput Aided Surg 2002;7(1):1–10.
[43] Finnis KW, Starreveld YP, Parrent AG, Sadikot AF, Peters TM. Three-dimensional database of subcortical electrophysiology for image-guided stereotactic functional neurosurgery. IEEE Trans Med Imaging 2003;22(1):93–104.
[44] Kall BA, Kelly PJ, Goerss S, Frieder G. Methodology and clinical experience with computed tomography and a computer-resident stereotactic atlas. Neurosurgery 1985; 17(3):400–7.
[45] St-Jean P, Sadikot AF, Collins L, Clonda D, Kasrai R, Evans AC, et al. Automated atlas integration and interactive three-dimensional visualization tools for planning and guidance in functional neurosurgery. IEEE Trans Med Imaging 1998;17(5):672–80.
[46] Metzger MC, Bittermann G, Dannenberg L, Schmelzeisen R, Gellrich NC, Hohlweg-Majert B, et al. Design and development of a virtual anatomic atlas of the human skull for automatic segmentation in computer-assisted surgery, preoperative planning, and navigation. Int J Comput Assist Radiol Surg 2013;8(5):691–702.
[47] Lehman RM, Micheli-Tzanakou E, Medl A, Hamilton JL. Quantitative on-line analysis of physiological data for lesion placement in pallidotomy. Stereotact Funct Neurosurg 2000;75(1):1–15.
[48] Collins DL, Holmes CJ, Peters TM, Evans AC. Automatic 3-D segmentation of neuroanatomical structures from MRI. Hum Brain Mapp 1995;3:190–208.
[49] Guo T, Parrent AG, Peters TM. Surgical targeting accuracy analysis of six methods for subthalamic nucleus deep brain stimulation. Comput Assist Surg 2007;12(6): 325–34.
[50] Guo T, Parrent AG, Peters TM. Automatic target and trajectory identification for deep brain stimulation (DBS) procedures. Med Image Comput Comput Assist Interv. In: Ayache N, OurselinS, editors. 10th International Conference, Brisbane, Australia. October 29–November 2. Proceedings Part I, LNCS 4791. Springer-Verlag: Berlin Heidelberg; 2007. p. 483–490.

[51] Tai CH, Wu RM, Lin CH, Pan MK, Chen YF, Liu HM, et al. Deep brain stimulation therapy for Parkinson's disease using frameless stereotaxy: comparison with frame-based surgery. Eur J Neurol 2010;17(11):1377–85.
[52] Garbelli R, Milesi G, Medicvi V, et al. Blurring in patients with temporal lobe epilepsy: clinical high-field and ultrastructure study. Brain 2012;135(Pt 8):2337–49.
[53] Khan AR, Goubran M, de Ribaupierre S, Hammond RR, Burneo JG, Parrent AG, et al. Quantitative relaxometry and diffusion MRI for lateralization in MTS and non-MTS temporal lobe epilepsy. Epilepsy Res 2014;108(3):506–16.
[54] Fisher R, Salanova V, Witt T, et al. SANTE Group. Electrical stimulation of the anterior nucleus of thalamus for treatment of refractory epilepsy. Epilepsia 2010; 51:899–908.
[55] Tykocki T, Mandat T, Kornakiewicz A, Koziara H, Nauman P. Deep brain stimulation for refractory epilepsy. Arch Med Sci 2012;8(5):805–16.
[56] Curry DJ, Gowda A, McNichols RJ, Wilfong AA. MR-guided stereotactic laser ablation of epileptogenic foci in children. Epilepsy Behav 2012;24(4):408–14.
[57] Iung B, Cachier A, Baron G, Messika-Zeitoun D, Delahaye F, Tornos P, et al. Decision-making in elderly patients with severe aortic stenosis: why are so many denied surgery? Eur Heart J 2005;26(24):2714–20.
[58] Haussig S, Schuler G, Linke A. Worldwide TAVI registries: what have we learned? Clin Res Cardiol 2014;103(8):603–12.
[59] Edwards Inc. http://www.edwards.com/products/transcathetervalve/pages/transapical.aspx.
[60] Siemens Inc. http://www.siemens.com/press/en/pressrelease/?press=/en/pressrelease/2010/healthcare/h201008050.htm.
[61] Philips Inc. http://www.healthcare.philips.com/de_de/products/interventional_xray/product/interventional_cardiac_surgery/interventional_tools/heartnavigator/.
[62] Luo Z, Cai J, Peters TM, Gu L. Intra-operative 2-D ultrasound and dynamic 3-D aortic model registration for magnetic navigation of transcatheter aortic valve implantation. IEEE Trans Med Imaging 2013;32(11):2152–65.
[63] McLeod AJ, Currie M, Moore J, Peters TM. Augmented reality guidance system for transcatheter aortic valve implantation. In: Proceedings of the 2nd international MICCAI workshop on computer assisted stenting; 2013.
[64] Chu MW, Moore J, Peters T, Bainbridge D, McCarty D, Guiraudon GM, et al. Virtual reality imaging with real-time ultrasound guidance for facet joint injection: a proof of concept. Anesth Analg 2010;110(5):1461–3.
[65] Rettmann ME, Holmes DR, Cameron BM, Robb RA. An event-driven distributed processing architecture for image-guided cardiac ablation therapy. Comput Methods Programs Biomed 2009;95(2):95–104.
[66] Linte CA, Lang P, Rettmann ME, Cho DS, Holmes 3rd DR, Robb RA, et al. Accuracy considerations in image-guided cardiac interventions: experience and lessons learned. Int J Comput Assist Radiol Surg 2012;7(1):13–25.
[67] Linte CA, Camp JJ, Holmes 3rd DR, Rettmann ME, Robb RA. Toward online modeling for lesion visualization and monitoring in cardiac ablation therapy. Med Image Comput Comput Assist Interv 2013a;16(Pt 1):9–17.